



Survey of ligand field parameters of strong field d^5 complexes obtained from the g matrix

Bruce R. McGarvey *

*Department of Chemistry and Biochemistry, University of Windsor, Windsor, Ont.,
Canada N9B 3P4*

Received 4 July 1997; accepted 3 November 1997

Contents

Abstract	75
1. Introduction	76
2. Strong field d^5 g matrix equations	76
2.1. Tetragonal distortion	76
2.1.1. d_{xy} , $d_{x^2-y^2}$, d_{z^2} basis set	76
2.1.2. d_{xy} , d_{xz} , d_{yz} basis set	79
2.2. Trigonal distortion	79
2.3. Cis complexes of MX_4Y_2	80
3. Application of equations to experimental results	81
3.1. Tetragonal hexa-monodentate complexes	82
3.2. Tetragonal mixed monodentates, bidentate complexes	85
3.3. Tetragonal Fe(III) porphyrin complexes	87
3.4. Trigonal complexes	89
4. Conclusions	91
Acknowledgements	91
References	92

Abstract

Using a newly proposed approach involving an internally consistent set of equations, the ligand field parameters Δ/ζ , V/ζ and k are obtained from literature values of the g matrix for strong field d^5 systems of various conformations in which $|A/\zeta| \leq 10$. Qualitative analysis of the observed results is done using the Angular Overlap Model, AOM. © 1998 Elsevier Science S.A.

Keywords: Angular overlap; Fe; g matrix; Ligand field; Os; Ru; Strong field d^5

* Tel: +1 519 253 4232; Fax: +1 519 973 7098; e-mail: beprm@uwindsor.ca

1. Introduction

Recently the theory and equations for the g matrix of strong field d^5 systems with small crystal field distortions relative to the one electron spin–orbit interaction parameter were reviewed and reexamined [1]. The literature is full of different equations that used different starting basis functions, different sign conventions, and, unfortunately in too many cases, contained errors. This has made it impossible to examine any systematic trends in some of the parameters that could be obtained through these equations from the large body of experimental g values in the literature. One of the things that kept many researchers from using any of the equations in the literature was the number of possible solutions that appeared necessary. The equations predicted various signs for each g value and since EPR cannot determine signs, it was considered necessary to consider all combinations. Further, most studies were done on frozen solutions so that it wasn't known which g value to assign to a given axis.

In the review [1] it was shown that the ambiguities in sign could be greatly reduced by using the boundary condition that in octahedral symmetry the three g values must be the same in magnitude and sign. The usual procedure of solving the equations using all possible sign combinations for the three principal g values was then not needed. The problem of labeling the g values was resolved by defining the z direction as the major distortion axis for the ligand field distortion of the t_{2g} orbitals and x and y by the minor energy distortion as has been done for many years for the zero field interaction and the quadrupole interaction. Thus one does not need to try all possible assignments to x , y and z . This mini-review will apply this approach to a variety of systems using the recent review article of Rieger [2] as a starting point and as a reference for much of the literature.

2. Strong field d^5 g matrix equations

Two distortions from octahedral symmetry have been considered; tetragonal and trigonal. For tetragonal distortions two separate basis sets have been used in most, if not all, treatments in the literature; d_{xy} , d_{+1} , d_{-1} or d_{xy} , d_{xz} , d_{yz} . The equations for the two distortions and two basis sets are summarized below. More details can be found in the review article [1]. In addition, it was found necessary during the course of writing this article to consider a third type of distortion that exists in the *cis* complexes of MX_4Y_2 with C_{2v} symmetry. Unlike the tetragonal distortion previously considered, this complex does not have all principal axes along the xyz bonding axes. Details for this are also included below.

2.1. Tetragonal distortion

2.1.1. d_{xy} , d_{+1} , d_{-1} basis set

The one electron ligand field energy parameters are defined as

$$\langle d_{xy} | H_C | d_{xy} \rangle = A; \quad \langle d_{xz} | H_C | d_{xz} \rangle = \frac{V}{2} = -\langle d_{yz} | H_C | d_{yz} \rangle \quad (1)$$

The requirement that the z direction be the major distortion axis is accomplished by requiring that $|A| \geq 2|V|/3$. The x and y axes are designated by the requirement that V and A are always of the same sign. The solution of the two energy matrices including the spin-orbit interaction is done using as basis functions

$$\begin{aligned} | -1, \pm \frac{1}{2} \rangle &= d_1^+ d_1^- d_{xy}^+ d_{xy}^- d_{\pm 1}^-; \quad | +1, \pm \frac{1}{2} \rangle = d_{\pm 1}^- d_{\pm 1}^- d_{xy}^+ d_{xy}^- d_1^{\pm}; \\ | 0, \pm \frac{1}{2} \rangle &= \pm i d_1^+ d_1^- d_{\pm 1}^- d_{\pm 1}^{\pm} \end{aligned} \quad (2)$$

This calculation gives a Kramer's doublet ground state that can be written as

$$\begin{aligned} \psi_- &= a| +1, -\frac{1}{2} \rangle + b| 0, \frac{1}{2} \rangle + c| -1, \frac{1}{2} \rangle \\ \psi_+ &= a| -1, \frac{1}{2} \rangle + b| 0, -\frac{1}{2} \rangle + c| +1, \frac{1}{2} \rangle \end{aligned} \quad (3)$$

and these two functions are then used to calculate the effective $S=1/2$ spin Hamiltonian that represents the behavior of the Zeeman energy of this doublet. This is the point where most of the inconsistencies in the literature have arisen. The subscripts of + and - given above indicate which function is assigned the $M_S = \pm 1/2$ quantum numbers in the derivation. Thus we have two possible results. What has often been overlooked is that although the magnitude and relative signs of a , b , c in Eq. (3) are obtained from the energy calculation, the relative phases of the two Kramer's doublet functions are not. That is, the sign of a , b , c in ψ_- could be the same as in ψ_+ or the opposite. We thus end up with four possible sets of equations for our three g values. These are listed in Table 1. Case 1a is for the labels of plus and minus to be assigned as shown in Eq. (3) above and the coefficients a , b , c to have the same sign in both functions. Case 2a is for the same assignment of plus and minus but the relative signs of a , b , c are opposite. Cases 1b and 2b have the plus and minus signs interchanged from 1a and 2a, respectively. It will be noted that equations for the four cases differ only in the signs of the three g values.

When one encounters more than one solution in a physical problem, one searches for boundary conditions in which one, hopefully, knows something about the correct physical result. Three boundary conditions come to mind. One is when A becomes positive and large and two is when it becomes negative and large in magnitude. In these two cases we should extrapolate to the free electron spin values of 2 for all three g values. The third boundary condition is for octahedral symmetry where $A=V=0$, in which case all three g values have to be equal by symmetry. Unfortunately,

Table 1
Equations for the g matrix for the four possible cases using the $d_{\pm 1}$ and d_{xy} basis functions for t_2

Case ^a	g_x	g_y	g_z
1a	$-2[-2ac + b^2 + k\sqrt{2}b(a-c)]$	$-2[2ac + b^2 + k\sqrt{2}b(a+c)]$	$-2[a^2 - b^2 + c^2 + k(a^2 - c^2)]$
2a	$-2[-2ac + b^2 + k\sqrt{2}b(a-c)]$	$2[2ac + b^2 + k\sqrt{2}b(a+c)]$	$2[a^2 - b^2 + c^2 + k(a^2 - c^2)]$
1b	$2[-2ac + b^2 + k\sqrt{2}b(a-c)]$	$2[2ac + b^2 + k\sqrt{2}b(a+c)]$	$-2[a^2 - b^2 + c^2 + k(a^2 - c^2)]$
2b	$2[-2ac + b^2 + k\sqrt{2}b(a-c)]$	$-2[2ac + b^2 + k\sqrt{2}b(a+c)]$	$2[a^2 - b^2 + c^2 + k(a^2 - c^2)]$

^a Defined in main text of article.

these three boundary conditions cannot be met simultaneously by any of the four cases considered. Only case 1a will meet the octahedral condition giving $g = -2$ for all three directions. The negative sign has actually been confirmed in a few systems by measuring the direction of rotation in the Larmor precession [3]. The equations for case 1a predict that g_x and g_y approach -2 for large positive values of Δ while g_z approaches $+2$. Therefore case 1b is needed to satisfy this boundary condition and this is the case adopted by perturbation treatments in this region. For large negative values of Δ and moderate values of V only case 2a would satisfy the boundary condition of all g 's equal to $+2$. Note, $V=0$ should not be considered because the Jahn–Teller theorem would predict a distortion. The fact that three different cases are needed to satisfy the three sets of boundary conditions is likely evidence of the inadequacy of the spin Hamiltonian representation for the system. I contend that one must use the boundary conditions closest to the system being represented and case 1a is the correct one for systems with small distortions from octahedral symmetry. The inconsistencies of most treatments in the literature come from ignoring all boundary conditions and choosing one of the four cases by pure whim.

It is reasonable to ask which case to choose in the intermediate regions but there is no correct answer. One could suggest the change occur at the value of Δ/ξ at which a g value changes sign but I would suggest that case 1a be used for $|\Delta/\xi| < 5$ and the case appropriate to the limiting conditions for large magnitudes of Δ for $|\Delta/\xi| > 5$. EPR only determines absolute values of g since $g = \sqrt{g_x^2 \sin^2 \theta \cos^2 \phi + g_y^2 \sin^2 \theta \sin^2 \phi + g_z^2 \cos^2 \theta}$. Experimental methods of determining the sign of g are generally limited to the three boundary condition regions since we need a magnetic moment that can freely precess. The only important condition is to treat your systems in a consistent manner.

The principal g matrix values are then

$$\begin{aligned} g_x &= -2[-2ac + b^2 + k\sqrt{2}b(a-c)] \\ g_y &= -2[2ac + b^2 + k\sqrt{2}b(a+c)] \\ g_z &= -2[a^2 - b^2 + c^2 + k(a^2 - c^2)] \end{aligned} \quad (4)$$

where k is the orbital reduction factor. The four parameters a , b , c and k can be obtained from Eq. (4) and the normalization condition $a^2 + b^2 + c^2 = 1$. It was shown that with the restrictions given above that there are only four possible assignments of the experimental g values. The largest and smallest g values, in magnitude, are either g_z, g_x , for $\Delta > 0$ or g_x, g_z for $\Delta < 0$, respectively. The intermediate g is always g_y . The largest two g values, in magnitude, are always negative, while the smallest in magnitude can be plus or minus. Two of these four assignments will violate the condition $|\Delta| \geq 2|V|/3$, so that only the two solutions appropriate to the two possible signs for either g_z or g_x will need to be considered. If you wish to know the values of Δ and V appropriate for an interchange of the labels x and z , they can be obtained from the conversion equations

$$\Delta' = -0.5\Delta - 0.75V; V' = 0.5V - \Delta$$

where the prime parameters are for the assignment where $|\Delta'| < 2|V'|/3$.

From the values of a , b , c and k , the values of Δ/ξ and V/ξ can be calculated from the following equations

$$\frac{\Delta}{\xi} = \frac{[b(1-b^2) + \sqrt{2}a(1-2a^2)]}{2b(a^2 - c^2)} \quad (5)$$

$$\frac{V}{\xi} = \frac{c(2a + \sqrt{2}b)}{(c^2 - a^2)} \quad (6)$$

where ξ is the single electron spin-orbit constant for the d^5 ion.

2.1.2. d_{xy} , d_{xz} , d_{yz} basis set

In this case the ground state Kramer's doublet is written for case 1a as

$$\begin{aligned} \psi_+ &= A|xy, \frac{1}{2}\rangle + B|yz, -\frac{1}{2}\rangle + C|xz, -\frac{1}{2}\rangle \\ \psi_- &= -A|xy, -\frac{1}{2}\rangle + B|yz, \frac{1}{2}\rangle - C|xz, \frac{1}{2}\rangle \end{aligned} \quad (7)$$

where

$$\begin{aligned} |xy, \pm \frac{1}{2}\rangle &= d_{xz}^+ d_{xz}^- d_{yz}^+ d_{yz}^- d_{xy}^{\pm} \\ |xz, \pm \frac{1}{2}\rangle &= i d_{yz}^+ d_{yz}^- d_{xy}^+ d_{xy}^- d_{xz}^{\pm} \\ |yz, \pm \frac{1}{2}\rangle &= d_{xz}^+ d_{xz}^- d_{xy}^+ d_{xy}^- d_{yz}^{\pm} \end{aligned} \quad (8)$$

Using the same definitions for the ligand field parameters and the assignment of the x , y and z axes, the g matrix equations become

$$\begin{aligned} g_x &= 2[B^2 - A^2 - C^2 - 2kAC] \\ g_y &= 2[C^2 - B^2 - A^2 - 2kAB] \\ g_z &= 2[A^2 - C^2 - B^2 - 2kBC] \end{aligned} \quad (9)$$

which are much more symmetrical than the equations proposed by Taylor [4], that are used by many researchers in the field. Conversion of Eq. (9) to Eq. (4) can be done with the equations

$$A = b; \quad B = \frac{(a+c)}{\sqrt{2}}; \quad C = \frac{(a-c)}{\sqrt{2}} \quad (10)$$

2.2. Trigonal distortion

We will only consider a trigonal distortion with a C_3 axis so all the systems will have axial symmetry. Since most of the systems with a trigonal distortion are tris-bidentates in which the bond angles are not 90° , we must consider the possibility of considerable configuration interaction with the t_{2g}^5 states. The Kramer's doublet for case 1a is now

$$\begin{aligned} \psi_+ &= a_i |+, -\frac{1}{2}\rangle + b_i |0, \frac{1}{2}\rangle \\ \psi_- &= -a_i |-, +\frac{1}{2}\rangle - b_i |0, -\frac{1}{2}\rangle \end{aligned} \quad (11)$$

where

$$|+, \pm \frac{1}{2}\rangle = t_2^-(+)t_2^+(-)t_2^-(-)t_2^+(0)t_2^-(0); \quad |-, \pm \frac{1}{2}\rangle = t_2^+(+)t_2^- (+)t_2^+(-)t_2^+(0)t_2^-(0);$$

$$|0, \pm \frac{1}{2}\rangle = t_2^-(+)t_2^-(+)t_2^+(-)t_2^-(-)t_2^{\pm}(0) \quad (12)$$

$$t_2(0) = d_0; \quad t_2(\pm) = \pm \alpha d_{-2} - \beta d_{\mp 1} \quad (13)$$

In octahedral symmetry $\alpha = \sqrt{2/3}$; $\beta = 1/\sqrt{3}$ and these are the usual values used in previous treatments but we should consider the possibility that this is not correct for the tris-bidentate complexes. Considerable distortion of the bond angles from 90° would allow σ interactions to add to the normal π interactions. In this distortion there is the one ligand distortion parameter $\Delta = \langle t_2(0) | H_C | t_2(0) \rangle$. The g matrix equations become

$$g_{\parallel} = 2[b_t^2 - a_t^2 - (2\alpha^2 - \beta^2)ka_t^2]; \quad g_{\perp} = 2[-b_t^2 - \sqrt{6}ka_t b_t \beta] \quad (14)$$

The sign of g_{\perp} is always negative for case Ia while g_{\parallel} can be either negative or positive when Δ/ξ is positive and larger than approximately one. Δ/ξ is obtained from the equation

$$\frac{\Delta}{\xi} = \frac{1}{2}(2 - 3\beta^2) + \frac{\sqrt{6}\beta(b_t^2 - a_t^2)}{2a_t b_t} \quad (15)$$

Unfortunately there are five unknowns a_t , b_t , α , β and k and only the four equations which are given by the two in Eq. (14) and the two normalization equations of $\alpha^2 + \beta^2 = 1$ and $a_t^2 + b_t^2 = 1$ and this has led most researchers to assume the octahedral values of α and β . We shall examine this problem below.

2.3. *Cis* complexes of MX_4Y_2

This system offers some difficulties in that one of the three principal axes falls along the bond axes. Since the principal g values must lie along symmetry axes, we must use d orbitals for the t_2 set appropriate to the symmetry axes rather than the bond axes. We shall choose as our z axis, the X–M–X axis because it offers the simplest transformation to convert orbitals to the bond axes system but will also turn out in most cases to be the axis for the major distortion of the t_2 orbital energies. That this is the major distortion axis is readily seen if we realize that in the bonding axes system, there are two planes with three X ligands plus one Y ligand and one with two X ligands plus two Y ligands. We have chosen the z axis to be perpendicular to the orbital in that plane since it should be different in energy from the other two orbitals. The x axis will be taken to be the C_2 axis bisecting the two M–Y bonds. The relationship between this xyz system and the bond axis system $x'y'z'$ is given by

$$d_{x^2-y^2} = d_{x'y'}; \quad d_{xz} = (1/\sqrt{2})[d_{x'z'} + d_{y'z'}]; \quad d_{yz} = (1/\sqrt{2})[-d_{x'z'} + d_{y'z'}]$$

We start with the following basis functions: $\vartheta_{B_1} = d_{xz}$, $\vartheta_{B_2} = id_{yz}$, $\vartheta_{A_1} = d_{x^2-y^2}$ and

define the parameters as

$$\langle \mathcal{G}_{A_1} | H_C | \mathcal{G}_{A_1} \rangle = A; \quad \langle \mathcal{G}_{B_2} | H_C | \mathcal{G}_{B_2} \rangle = \frac{V}{2} = -\langle \mathcal{G}_{B_1} | H_C | \mathcal{G}_{B_1} \rangle \quad (16)$$

If we now write the full d^5 functions as

$$\begin{aligned} |x^2 - y^2, \pm \frac{1}{2}\rangle &= \mathcal{G}_{B_1}^+ \mathcal{G}_{B_1}^- \mathcal{G}_{B_2}^+ \mathcal{G}_{B_2}^- \mathcal{G}_{A_1}^\pm; & |xz, \pm \frac{1}{2}\rangle &= \mathcal{G}_{B_2}^+ \mathcal{G}_{B_2}^- \mathcal{G}_{A_1}^+ \mathcal{G}_{A_1}^- \mathcal{G}_{B_1}^\pm; \\ |yz, \pm \frac{1}{2}\rangle &= i\mathcal{G}_{B_1}^+ \mathcal{G}_{B_1}^- \mathcal{G}_{A_1}^+ \mathcal{G}_{A_1}^- \mathcal{G}_{B_2}^\pm \end{aligned} \quad (17)$$

we obtain two energy matrices identical to those obtained in the tetragonal distortion for the d_{xy} , d_{xz} , d_{yz} basis set, except $|xz, \pm 1/2\rangle$ and $|yz, \pm 1/2\rangle$ are interchanged. We thus obtain for the Kramer's doublet

$$\begin{aligned} \psi_- &= A|xy, \frac{1}{2}\rangle + B|xz, -\frac{1}{2}\rangle + C|yz, -\frac{1}{2}\rangle \\ \psi_+ &= -A|xy, -\frac{1}{2}\rangle + B|xz, \frac{1}{2}\rangle - C|yz, \frac{1}{2}\rangle \end{aligned} \quad (18)$$

and for the g values

$$\begin{aligned} g_x &= 2[B^2 - A^2 - C^2 - 2kAC] \\ g_y &= 2[C^2 - B^2 - A^2 - 2kAB] \\ g_z &= 2[A^2 - C^2 - B^2 - 2kBC] \end{aligned} \quad (19)$$

Thus we can use the same tetragonal equations but assign the coefficients A , B , C to slightly different functions.

The C_{2v} symmetry allows for configurational interaction such that the A_1 function can be written as $\mathcal{G}_{A_1} = a d_{x^2-y^2} + b d_{z^2}$. If this form is used, the g_x term in Eq. (19) has the k multiplied by $(a + \sqrt{3}b)$ and k in g_y is multiplied by $(a - \sqrt{3}b)$.

3. Application of equations to experimental results

For tetragonal distortions a simple program has been written [1] to solve Eqs. (4)-(6) for tetragonal distortions given the absolute g values and using the sign conventions and coordinate assignments outlined earlier. Eq. (10) can be used to obtain the orbital parameters for the other basis set of d_{xy} , d_{xz} , d_{yz} . A similar program has also been written for the trigonal case.

Most of the g values in the literature were obtained from either powder or frozen solution spectra and cannot be considered very accurate or reliable. They are reasonably good if the line widths are narrow and one can easily resolve the three g regions but this is not often the case. The best method to extract the g values is to use a simulation program to fit with the experimental spectrum but this has not been done in most of the literature on d^5 systems. In fact most literature references never tell us how the g values were extracted and do not show the spectra, and one often suspects the method was not very good. In fact there are examples, when a spectrum is shown, where it can be seen that the g values were chosen incorrectly. One example, of many, is in the paper by Araneo *et al.* [5] where it is clear that the

method of choosing the intermediate g value is wrong. All of the above discussion has been given as a warning that the values of Δ/ξ , V/ξ and k given below may be very approximate.

For the qualitative analysis of the signs and magnitudes of the values for Δ/ξ and V/ξ found from the calculations, the Angular Overlap Model [6–9], AOM, will be employed. Use of this simple model seems to explain most of the features observed.

3.1. Tetragonal hexa-monodentate complexes

We first consider representative examples of complexes with six monodentate ligands which can be reasonably treated as typical tetragonal distortions. In Table 2 are given the two solutions, with the result having the smaller k value given first, for a selected group of complexes. These fall into the categories of MX_6 , MX_5Y , *trans*- and *cis*- MX_4Y_2 , *trans*- MX_4YZ , and *mer*- MX_3Y_3 . The *fac*- MX_3Y_3 are trigonal in symmetry and are listed in Table 5 with the trigonal complexes. The asterisk indicates the favored solution. The reasons for the choice will become apparent in the following discussion, but in general it is determined by a combination of the value of k and the reasonableness of the magnitude of Δ/ξ and V/ξ . In the following discussions, the following values will be taken for the single electron spin-orbit parameter ξ : $\xi(\text{Fe}^{3+}) = 400 \text{ cm}^{-1}$, $\xi(\text{Ru}^{3+}) = 1000 \text{ cm}^{-1}$, $\xi(\text{Os}^{3+}) = 3000 \text{ cm}^{-1}$.

An examination of the table reveals the following general features. The supposedly octahedral complexes are all distorted to give three different g values which can be attributed to the static Jahn–Teller distortion of the degenerate ${}^2\text{T}_{2g}$ ground state. The fourfold symmetry ($V=0$) of the MX_5Y and *trans*- MX_4Y_2 complexes is found when Δ/ξ is positive but is missing when Δ/ξ is negative. Again this can be attributed to a static Jahn–Teller distortion of the ${}^2\text{E}_g$ ground state for the ion when Δ/ξ is negative. The *mer*- MX_3Y_3 , which have a C_{2v} symmetry, have magnitudes for V/ξ that are sizable as might be expected. Since we designate the principal coordinate system by the crystal field distortions, we don't know where the z axis is relative to the molecular axes except for those that exhibit axial symmetry. The single crystal study [12] for $[\text{Fe}(\text{CN})_5\text{NH}_3]^{2-}$ found the z axis to be the Fe– NH_3 bond axis but the single crystal study [18] of *mer*- $\text{Os}(\text{Pbu}_2\text{Et})_3\text{Cl}_3$ found the z axis for the complex to be perpendicular to the C_2 axis of the molecule close to the Cl–Os–Cl axis.

In the AOM treatment of these systems, we recognize that the d orbitals that have unpaired electrons interact with the ligand orbitals in a π fashion. The energy of interaction for the antibonding d orbitals with one ligand atom will be represented by the symbol ϵ_π . Thus if we take the z axis to be the M–Y axis for the MX_5Y and *trans*- MX_4YZ complexes the energy of the three d orbitals will be

$$E(xy) = 4\epsilon_\pi(X); \quad E(xz) = E(yz) = 2\epsilon_\pi(X) + \epsilon_\pi(Y) + \epsilon_\pi(Z) \quad (20)$$

giving

$$\begin{aligned} \Delta &= [\epsilon_\pi(X) - \epsilon_\pi(Y)] \text{ (for } \text{MX}_5\text{Y) and} \\ \Delta &= 2\epsilon_\pi(X) - \epsilon_\pi(Y) - \epsilon_\pi(Z) \text{ (for } \text{MX}_4\text{YZ)} \end{aligned} \quad (21)$$

Table 2
Tetragonal hexa-monodentate complexes

Complex	g_x	g_y	g_z	a	b	c	d/ξ	V/ξ	k	Ref.
$[\text{Fe}(\text{CN})_6]^{3-}$	-2.35	-2.10	0.915	0.4591	0.8875	-0.0384	1.518	0.399	0.564	[10]
*	-2.35	-2.10	-0.915	0.7116	0.7021	-0.0272	0.484	0.130	0.877	
$[\text{Ru}(\text{NH}_3)_6]^{3+}$	-2.21	-2.05	1.50	0.3219	0.9461	-0.0341	2.373	0.661	0.394	[11]
*	-2.21	-2.05	-1.50	0.7703	0.6374	-0.0167	0.231	0.069	0.949	
$[\text{Fe}(\text{CN})_5(\text{NH}_3)]^{2-}$	0.845	-2.177	-2.995	0.9020	0.2408	0.3582	-1.727	-1.121	0.895	[12]
Single crystal	-0.845	-2.177	-2.995	0.8968	0.4208	0.1365	-0.644	-0.415	1.084	
$[\text{Ru}(\text{NH}_3)_5\text{Cl}]^{2+}$	0.987	-1.513	-2.983	0.6413	0.1295	0.3118	-4.407	-0.817	0.666	[13]
Single crystal *	-0.987	-1.513	-2.983	0.9200	0.3880	0.0558	-0.874	-0.158	0.940	
$[\text{Ru}(\text{NH}_3)_5\text{Br}]^{2+}$	1.13	-1.634	-2.798	0.9262	0.1375	0.3511	-3.973	-0.979	0.595	[13]
Single crystal *	-1.13	-1.634	-2.798	0.9032	0.4259	0.0532	-0.662	-0.158	0.937	
$[\text{Os}(\text{NH}_3)_5\text{Cl}]^{2+}$	1.47	-1.69	-2.41	0.5985	0.0989	0.4276	-5.528	-1.327	0.360	[11]
*	-1.47	-1.69	-2.41	0.8708	0.4912	0.0232	-0.354	-0.075	0.907	
<i>trans</i> - $[\text{Ru}(\text{NH}_3)_4\text{Cl}_2]^+$	1.18	-1.54	-3.33	0.9352	0.0717	0.3467	-8.504	-0.906	0.895	[14]
Single crystal *	-1.18	-1.54	-3.33	0.9267	0.3740	0.0369	-0.965	-0.103	1.102	
<i>trans</i> - $[\text{Ru}(\text{PEt}_3)_2\text{Cl}_4]^-$	-2.51	-2.51	1.64	0.2478	0.9688	0.0000	3.084	0.000	0.932	[15]
*	-2.51	-2.51	-1.64	0.7563	0.6542	0.0000	1.182	0.000	1.182	
<i>trans</i> - $[\text{Ru}(\text{AsPh}_3)_2\text{Cl}_4]^-$	-2.49	-2.49	1.73	0.2126	0.9771	0.0000	3.597	0.000	0.988	[16]
*	-2.49	-2.49	-1.73	0.7646	0.6445	0.0000	0.257	0.000	1.190	
<i>trans</i> - $[\text{Os}(\text{CO})(\text{py})\text{Cl}_4]^-$	-2.55	-2.55	1.72	0.2129	0.9771	0.0000	3.591	0.000	1.089	[17]
*	-2.55	-2.55	-1.72	0.7600	0.6500	0.0000	0.228	0.000	1.220	
<i>trans</i> - $[\text{Os}(\text{CO})(\text{py})\text{Br}_4]^-$	-2.50	-2.50	1.80	0.1786	0.9839	0.0000	4.267	0.000	1.134	[17]
*	-2.50	-2.50	-1.80	0.7692	0.6390	0.0000	0.236	0.000	1.211	
<i>trans</i> - $[\text{Os}(\text{CO})(\text{py})\text{I}_4]^-$	-2.31	-2.31	1.93	0.1060	0.9944	0.0000	7.058	0.000	1.115	[17]
*	-2.31	-2.31	-1.93	0.7910	0.6118	0.0000	0.133	0.000	1.141	
<i>trans</i> - $[\text{Os}(\text{CO})_2\text{Br}_4]$	-2.46	-2.46	1.81	0.1761	0.9844	0.0000	4.327	0.000	1.065	[17]
*	-2.46	-2.46	-1.81	0.7726	0.6349	0.0000	0.221	0.000	1.192	
<i>trans</i> - $[\text{Os}(\text{CO})_2\text{I}_4]^-$	-2.32	-2.32	1.92	0.1140	0.9935	0.0000	6.584	0.000	1.080	[17]
*	-2.32	-2.32	-1.92	0.7896	0.6136	0.0000	0.140	0.000	1.144	
<i>mer</i> - $\text{Ru}(\text{PMe}_2\text{Ph})_3\text{Cl}_3$	1.66	-2.03	-2.99	0.8594	0.0690	0.5066	-7.69	-1.909	1.047	[15]
*	-1.66	-2.03	-2.99	0.8826	0.4687	0.0361	-0.454	-0.113	1.201	
<i>mer</i> - $\text{Ru}(\text{SMePh})_3\text{Cl}_3$	-2.70	-2.29	1.68	0.2299	0.9715	-0.0576	3.587	2.130	0.961	[15]
*	-2.70	-2.29	-1.68	0.7598	0.6490	-0.0393	0.280	0.166	1.185	
<i>mer</i> - $\text{Os}(\text{PBu}_2\text{Ph})_3\text{Cl}_3$	0.32	-1.44	-3.32	0.9571	0.2061	0.2035	-2.578	-0.513	0.852	[18]
Single crystal *	-0.32	-1.44	-3.32	0.9501	0.2867	0.1230	-1.609	-0.319	0.929	

Applying this to the MX_5Y complexes and assuming that $\epsilon_\pi(\text{NH}_3) \approx 0$, we obtain for $[\text{Fe}(\text{CN})_5\text{NH}_3]^{2-}$ $\Delta = \epsilon_\pi(\text{CN}) = -690 \text{ cm}^{-1}$, assuming the best solution is that with the smaller k value. The negative sign for $\epsilon_\pi(\text{CN})$ would be due to π back bonding into the LUMO orbital of CN^- making the cyanide ion a π acceptor ligand. For the complexes with $\text{X} = \text{NH}_3$, we obtain $\epsilon_\pi = 870 \text{ cm}^{-1}$ for Cl^- and 660 cm^{-1} for Br^- in ruthenium(III) complexes and $\epsilon_\pi = 1000 \text{ cm}^{-1}$ for Cl^- in the osmium(III) complex. These are reasonable values for ϵ_π for the halides as π donors.

We now consider the MX_4YZ complexes, which require the second form of Eq. (21). For $\text{trans-}[\text{Ru}(\text{NH}_3)_4\text{Cl}_2]^+$ the solution chosen is the one with a k value larger than unity because the other solution has an unreasonably large value of Δ . This complex gives $\epsilon_\pi = 480 \text{ cm}^{-1}$ which is smaller than that obtained from the MX_5Y complexes but this could be justified by noting that this complex has two negative chlorides donating electrons into the same d orbitals. The other complexes of this type all have $\text{X} = \text{halide ion}$ and a positive value for Δ . The positive value means that the ϵ_π of the halide must be more positive than that of the *trans* ligands. In the case of $\text{trans-}[\text{Ru}(\text{PET}_3)_2\text{Cl}_4]^-$, we get a value for $\epsilon_\pi(\text{Cl}^-)$ about half of that obtained from $\text{trans-}[\text{Ru}(\text{NH}_3)_4\text{Cl}_2]^+$ indicating that ϵ_π for PET_3 is small. Using similar arguments for the others required us to choose, as the correct solution, the one with $k = 1.1\text{--}1.2$ rather than the ones with $k \approx 1$ which give an unrealistically large value for Δ . The similar values of Δ for related complexes having two *trans* CO ligands versus those with one CO and one py ligand would suggest similar values of ϵ_π for both of these ligands.

There are no *cis*- MX_4Y_2 (C_{2v} symmetry) complexes in the table but it is of interest to see what the AOM approach would predict. Using the coordinate system defined earlier in Section 2.3 and remembering that the d_{xz} and d_{yz} orbitals in this system are linear combinations of the $d_{x'z'}$ and $d_{y'z'}$ orbitals in the bond axis system, we obtain for the d orbital energies

$$E(xy) = 2\epsilon_\pi(\text{X}) + 2\epsilon_\pi(\text{Y}); \quad E(xz) = E(yz) = 3\epsilon_\pi(\text{X}) + \epsilon_\pi(\text{Y}) \quad (22)$$

and therefore

$$\Delta = \epsilon_\pi(\text{Y}) - \epsilon_\pi(\text{X}); \quad V = 0 \quad (23)$$

This predicts an apparent axial symmetry in the g matrix but the z axis is perpendicular to the C_2 axis of the complex.

The *mer*- MX_3Y_3 complexes which also have C_{2v} symmetry with the C_2 axis being the X-M-Y axis. The other two axes are X-M-X and Y-M-Y . If we try the C_2 axis as z we obtain the energies

$$\begin{aligned} E(xy) &= 2\epsilon_\pi(\text{X}) + 2\epsilon_\pi(\text{Y}); & E(xz) &= 3\epsilon_\pi(\text{X}) + \epsilon_\pi(\text{Y}); \\ E(yz) &= \epsilon_\pi(\text{X}) + 3\epsilon_\pi(\text{Y}) \end{aligned} \quad (24)$$

which would give $\Delta = 0$, $V = 2[\epsilon_\pi(\text{X}) - \epsilon_\pi(\text{Y})]$. Since this is an unacceptable solution, we must choose the z axis to be perpendicular to C_2 . Interchanging the labels x and z in Eq. (24) will give $\Delta = 3[\epsilon_\pi(\text{Y}) - \epsilon_\pi(\text{X})]/2$; $V = [\epsilon_\pi(\text{Y}) - \epsilon_\pi(\text{X})]$; and $V/\Delta = 2/3$. It is pleasing to note that the z axis is perpendicular to C_2 in the one system studied

in a single crystal [18]. V/Δ is close to $2/3$ for the *mer*-Ru(SMePh)₃Cl₃ complex and near 0.25 for the two phosphine-like ligands in Table 2. $V/\Delta \neq 2/3$ comes about when ϵ_π for the axial ligands are different from that of the same ligands in the equatorial positions.

3.2. Tetragonal mixed monodentates, bidentate complexes

In Table 3 are listed the results for complexes that have one or two bidentate ligands in a six coordinate complex. The quadridentate cyclam complexes have been included as it is basically two ethylene-diammine, en, complexes fused into a ring structure. Attempts to explain the results in terms of π interactions only, as was done above for the complexes with monodentate ligands, is not expected to be as successful since the bite angle could be different from 90° resulting in σ interactions becoming significant.

We have put no asterisk to indicate a choice as to the best of the two solutions. All of the solutions that have a k value closest to or below unity have the largest value of Δ/ξ which in many cases for the ruthenium complexes gives unreasonably high values for Δ . Unfortunately, there are no single crystal studies among these systems to give us an idea as to the location of the principal axes relative to the molecular axes in these low symmetry complexes.

The first three complexes in the table have only one bidentate ligand and are necessarily *cis* in conformation. If only π interactions are important and are dominated by $\epsilon_\pi(\text{CN})$, Eq. (23) would predict that Δ is positive and V is small in magnitude. This is true except for $[\text{Fe}(\text{en})(\text{CN})_4]^-$, which means that the largest distortion for this complex is along an axis perpendicular to that of the other two complexes. If we were to use the same xyz axes that were used for the other two (namely, $g_x = -3.15$, $g_y = -1.99$, $g_z = \pm 0.82$), $(\Delta/\xi, V/\xi)$ would become (1.850, 2.730) and (0.670, 0.638) for the two solutions, respectively. Apparently, the ethylene-diammine ligand causes considerable distortion from octahedral geometry. The few significant figures for g and the large values for k leads us to suspect that the $V=0.0$ for $[\text{Fe}(\text{phen})(\text{CN})_4]^-$ is the result of an incorrect determination of the three g values.

The five complexes in Table 3 with a *trans* conformation have equatorial ligands with $\epsilon_\pi \approx 0$ which according to Eq. (21) should give a negative Δ of similar magnitude for all of them. The positive value for *trans*- $[\text{Ru}(\text{en})_2\text{Br}_2]^+$ is probably the result of en distorting the energy system more in the plane perpendicular to the Br–Ru–Br axis. If we interchange the x and z labels, $(\Delta/\xi, V/\xi)$ would become (–1.704, –1.339) and (–0.546, –0.427) for the two solutions, respectively.

The last four *cis* complexes in Table 3 which have two bidentate ligands can be approximated as a *cis* MX_4Y_2 system for which we use Eq. (23). Since the Y ligand is the major π bonding ligand we would expect a positive value for Δ . Three of the four do have a positive value, at least. The symmetry is C_2 at best for these complexes, so distortions of bonding axes from 90° could result in configuration mixing with the e_g orbitals and this may explain the results for *cis*- $[\text{Ru}(\text{dmpe})_2\text{Cl}_2]^+$.

Table 3
Tetragonal mixed monodentates, bidentate complexes

Complex	g_x	g_y	g_z	a	b	c	d/ξ	V/ξ	k	Ref.
$[\text{Fe}(\text{en})(\text{CN})_4]^-$ *	0.82	-1.99	-3.15	0.9189	0.2108	0.3333	-2.244	-0.971	0.905	[19]
	-0.82	-1.99	-3.15	0.9116	0.3929	0.1206	-0.813	-0.351	1.082	
$[\text{Fe}(\text{bpy})(\text{CN})_4]^-$ *	-2.50	-2.30	1.65	0.2504	0.9676	-0.0322	3.112	0.975	0.770	[20]
	-2.50	-2.30	-1.65	0.7641	0.6448	-0.0196	0.260	0.082	1.125	
$[\text{Fe}(\text{phen})(\text{CN})_4]$ *	-2.7	-2.7	1.6	0.2498	0.9683	0.0000	3.059	0.000	1.206	[20]
	-2.7	-2.7	-1.6	0.7411	0.6714	0.0000	0.360	0.000	1.278	
<i>trans</i> - $[\text{Ru}(\text{en})_2\text{Cl}_2]^+$	1.11	-2.25	-3.14	0.893	0.1925	0.4071	-2.325	-1.327	1.020	[14]
*	-1.11	-2.25	-3.14	0.8949	0.4317	0.1131	-0.603	-0.344	1.196	
<i>trans</i> - $[\text{Ru}(\text{en})_2\text{Br}_2]^+$	-3.02	-2.36	0.99	0.4086	0.9093	-0.0791	1.856	1.035	0.986	[21]
	-3.02	-2.36	-0.99	0.6863	0.7244	-0.0643	0.592	0.330	1.166	
<i>trans</i> - $[\text{Ru}(\text{dmpe})_2\text{Cl}_2]^+$ *	1.57	-1.88	-3.18	0.8829	0.0561	0.4662	-10.173	-1.530	1.061	[15]
	-1.57	-1.88	-3.18	0.8986	0.4376	0.0305	-0.606	-0.091	1.206	
$[\text{Fe}(\text{cyclam})\text{Cl}_2]^+$ *	1.15	-2.23	-3.26	0.5952	0.1737	0.4105	-2.705	-1.321	1.091	[22]
	-1.15	-2.23	-3.26	0.8999	0.4230	0.1063	-0.653	-0.319	1.237	
$[\text{Ru}(\text{cyclam})\text{Cl}_2]^+$	1.16	-1.95	-3.18	0.9108	0.1468	0.3859	-3.528	-1.151	0.930	[23]
*	-1.16	-1.95	-3.18	0.9069	0.4138	0.080	-0.717	-0.234	1.142	
<i>cis</i> - $[\text{Fe}(\text{bpy})_2(\text{CN})_2]^-$ *	-2.74	-2.47	1.54	0.2755	0.9607	-0.0350	2.820	0.895	1.014	[24]
	-2.74	-2.47	-1.54	0.7420	0.6700	-0.0256	0.357	0.113	1.214	
<i>cis</i> - $[\text{Fe}(\text{phen})_2(\text{CN})_2]^-$ *	-2.63	-2.63	1.42	0.3117	0.9502	0.0000	2.423	0.000	0.984	[24]
	-2.63	-2.63	-1.42	0.7307	0.6828	0.0000	0.404	0.000	1.203	
<i>cis</i> - $[\text{Ru}(\text{en})_2\text{Cl}_2]^+$ *	-2.82	-2.41	1.02	0.4094	0.9109	-0.0516	1.797	0.659	0.906	[21]
	-2.82	-2.41	-1.02	0.6950	0.7178	-0.0405	0.552	0.202	1.123	
<i>cis</i> - $[\text{Ru}(\text{dmpe})_2\text{Cl}_2]^+$ *	1.88	-2.13	-2.59	0.7992	0.0496	0.5990	-9.519	-3.572	1.072	[15]
	-1.88	-2.13	-2.59	0.8523	0.5224	0.0244	-0.219	-0.082	1.159	

3.3. Tetragonal Fe(III) porphyrin complexes

We now come to the model porphyrin complexes. In Table 4 are listed some of the results for these systems. Most of the complexes in the table involve tetraphenyl porphyrin, TPP, which has a fourfold symmetry but all of the complexes in the table have $V \neq 0$, which has to come from either the lower symmetry of the axial ligands or a Jahn–Teller distortion of TPP. If we had only TPP bonded to the iron atom and take the z axis perpendicular to the TPP plane, the AOM model would give

$$E(xz) = E(yz) = 2\epsilon_{\pi}(\text{TPP}); \quad E(xy) = 0 \quad (25)$$

$$\Delta = -2\epsilon_{\pi}(\text{TPP}); \quad V = 0 \quad (26)$$

A negative value for Δ would give a degenerate 2E state which should distort according to the Jahn–Teller theorem to a tetragonal symmetry. Many of the complexes in Table 4 have two ligands bonded along the z axis that are aromatic and capable of π bonding, mainly through their conjugated π system. Strouse and co-workers [28] have proposed a model for these systems to explain Δ and V . If we assign the x axis to be in the plane of the axial ligand, we add $2\epsilon_{\pi}(a)$ to $E(yz)$ in Eq. (21), if both axial ligands are oriented in the same plane. This then gives for Δ and V

$$\Delta = -2\epsilon_{\pi}(\text{TPP}) - \epsilon_{\pi}(a); \quad V = -2\epsilon_{\pi}(a) \quad (27)$$

If $\epsilon_{\pi}(\text{TPP}) = \epsilon_{\pi}(a)$, V/Δ would be $2/3$ and if $\epsilon_{\pi}(\text{TPP}) < \epsilon_{\pi}(a)$, we would find that the z axis, as defined in this work, would be found in the porphyrin plane. Note that, in this model, the axial distortion would disappear if the two axial ligands were oriented perpendicular to each other.

Single crystal studies [27] have shown that for $[\text{Fe}(\text{TPP})(\text{py})_2]^+$ and $[\text{Fe}(\text{TPP})(\text{CN})_2]^-$ that the z axis in Table 4 is perpendicular to the porphyrin plane while the x and y axes are between the two nitrogen atoms of the porphyrin for the py complex and near the Fe–N axes for the CN complex. The above model does not apply to the CN complex because there is no anisotropy in the π interaction of the CN^- ion. For this complex, the AOM model would predict axial symmetry with $\Delta = -2[\epsilon_{\pi}(\text{TPP}) + \epsilon_{\pi}(a)]$. The similarity in Δ and V for both of these complexes would suggest that $\epsilon_{\pi}(a)$ is small for both CN^- and py in these porphyrin complexes and the V is primarily due to other distortions. The solution with the larger k value is favored because the Δ value for the other solution is unreasonably large. The very different result [25] for $[\text{Fe}(\text{TPP})(\text{py})_2]^+$ in frozen solution from the single crystal result is due to the fact that the g_y listed in the table was estimated from the other two by assuming the sum of the squares of the g values is 16, which apparently is not a reliable method, particularly for solution systems in which the other g values were poorly determined.

Explaining the other single crystal result for $[\text{Fe}(\text{TPP})(\text{SPh})_2]^-$ is difficult. The ease of detection at higher temperatures, 160 K, favors $\Delta/\xi = 10.3$ but this gives a $k = 1.36$ and Δ and V values much too large to explain in terms of an AOM model

Table 4
Fe(III) porphyrin and related complexes

Complex	g_x	g_y	g_z	a	b	c	A/ξ	V/ξ	k	Ref.
[Fe(TPP)(4-NH ₂ py) ₂] ⁺ *	1.603	2.289	-2.830	0.8448	0.1285	0.5195	-3.368	-2.191	1.010	[25]
[Fe(TPP)(pyrazole) ₂] ⁻ *	-1.603	-2.289	-2.830	0.8673	0.4933	0.0666	-0.333	-0.217	1.206	[25]
[Fe(TPP)(s-triazine) ₂] ⁺ *	-2.615	-2.378	1.714	0.2179	0.9754	-0.0330	3.604	1.289	0.987	[25]
[Fe(TPP)(s-triazine) ₂] ⁺ *	-2.615	-2.378	-1.714	0.7627	0.6463	-0.0227	0.266	0.095	1.191	[25]
[Fe(TPP)(Im) ₂] ⁻ *	-2.747	-2.284	1.646	0.2412	0.9684	-0.0640	3.453	2.190	0.969	[25]
[Fe(TPP)(Im) ₂] ⁻ *	1.563	-2.287	-2.869	0.8506	0.1340	0.5085	-3.260	-2.068	1.012	[25]
[Fe(TPP)(N-MeIm) ₂] ⁻ *	-1.563	-2.287	-2.869	0.8704	0.4874	0.0703	-0.358	-0.227	1.209	[25]
[Fe(TPP)(N-MeIm) ₂] ⁻ *	1.549	-2.294	-2.886	0.8520	0.1363	0.5054	-3.202	-2.038	1.021	[25]
[Fe(TPP)(2-MeIm) ₂] ⁻ *	-1.549	-2.294	-2.886	0.8713	0.4854	0.0723	-0.366	-0.233	1.212	[25]
[Fe(TPP)(2-MeIm) ₂] ⁻ *	1.188	-1.74	-3.399	0.9245	0.0982	0.3682	-5.879	-1.018	0.999	[25]
[Fe(TPP)(2-MeIm) ₂] ⁻ *	-1.188	-1.74	-3.399	0.9221	0.3830	0.0557	-0.904	-0.157	1.172	[25]
[Fe(TPP)(py) ₂] ⁺ *	1.05	-2.36	-3.48	0.8970	0.1842	0.4019	-2.510	-1.284	1.256	[26]
[Fe(TPP)(py) ₂] ⁺ *	-1.05	-2.36	-3.48	0.9055	0.4048	0.1274	-0.739	-0.378	1.328	[26]
[Fe(PPIX)(py) ₂] ⁺ *	1.2	-1.7	-3.4	0.9261	0.0901	0.3665	-6.499	-1.003	0.990	[25]
[Fe(PPIX)(py) ₂] ⁺ *	-1.2	-1.7	-3.4	0.9232	0.3810	0.0505	-0.142	-0.142	1.166	[26]
[Fe(TPP)(py) ₂] ⁺ *	0.98	-2.25	-3.43	0.9053	0.1889	0.3806	-2.495	-1.172	1.166	[26]
Crystal, ClO ₄ salt *	-0.98	-2.25	-3.43	0.9091	0.3974	0.1254	-0.783	-0.368	1.272	[26]
[Fe(TPP)(CN) ₂] ⁻ *	0.46	-1.12	-3.70	0.9755	0.1150	0.1875	-5.372	-0.432	0.956	[27]
Crystal, K salt *	-0.46	-1.12	-3.70	0.9684	0.2388	0.0722	-2.087	-0.176	1.034	[27]
[Fe(TPP)(SPh) ₂] [*]	0.52	-1.05	-3.70	0.9775	0.0947	0.1886	-6.688	-0.428	0.944	[27]
Crystal, K salt *	-0.52	-1.05	-3.70	0.9695	0.2381	0.0580	-2.201	-0.141	1.029	[27]
[Fe(TPP)(tht) ₂] ⁻ *	-2.336	-2.215	1.962	0.0749	0.9971	-0.0146	10.268	4.229	1.359	[28]
Crystal, K salt *	-2.336	-2.215	-1.962	0.7955	0.6059	-0.0118	0.1106	0.046	1.131	[28]
Fe(OEP)(tht)(SPh) *	-2.38	-2.27	-1.93	0.7900	0.6130	-0.0107	0.138	0.042	1.149	[29]
[Fe(TPP)(tht) ₂] ⁻ *	-2.38	-2.27	1.93	0.1046	0.9944	-0.0147	7.301	2.215	1.180	[29]
[Fe(TPP)(tht) ₂] ⁻ *	-2.89	-2.37	1.46	0.2967	0.9527	-0.0661	2.722	1.534	1.019	[30]
[Fe(TPP)(tht) ₂] ⁻ *	-2.89	-2.37	-1.46	0.7331	0.6783	-0.0494	0.398	0.224	1.216	[30]
[Fe(PC)(OH) ₂] [*]	1.96	-2.11	-2.31	0.7602	0.0337	0.6488	-12.634	-6.485	1.002	[31]
[Fe(PC)(OH) ₂] [*]	-1.96	-2.11	-2.31	0.8341	0.5514	0.0149	-0.102	-0.052	1.097	[31]

involving π interactions only. A similar problem of interpretation occurs with the $[\text{Fe}(\text{PC})(\text{OH})_2]^-$ complex in which high temperature detection favors the larger magnitude Δ and V values.

Most of the TPP complexes with aromatic ligands fit the AOM theory given above with Δ negative and large values of V , some approaching $V/\Delta=2/3$. The positive sign for Δ for $[\text{Fe}(\text{TPP})(\text{pyrazole})_2]^+$ and $[\text{Fe}(\text{TPP})(s\text{-triazine})_2]^+$ are simply cases where the major distortion direction has switched into the porphyrin plane. The values of Δ/ξ and V/ξ for z being perpendicular to the plane of these two complexes are $(-2.769, -2.960)$ and $(-3.369, -2.358)$, respectively. The favored solution in Table 4 for these complexes is the one with the larger Δ value, because many of these complexes have been detected easily at 100 K. In most cases this is the solution with k closer to unity.

The positive values of Δ for the three complexes with the sulfur ligands PhS^- and tht , tetrahydrothiophene, would suggest $\epsilon_x(\text{S})$ is large and negative but the large magnitude for PhS^- seems too large to be reasonable. Perhaps other distortions bringing in sigma interactions are present in these systems.

3.4. Trigonal complexes

Analyses of these trigonal complexes assuming $\alpha=\sqrt{2/3}$; $\beta=1/\sqrt{3}$, are given in Table 5. In the case of $[\text{Os}(\text{bpy})_3]^{3+}$ and $[\text{Os}(\text{phen})_3]^{3+}$ g_{\parallel} was not detected but its magnitude was estimated to be less than 0.4 and that is the value used in the calculations. There is little difference between the $g_{\parallel}=\pm 0.40$ solutions. It is difficult to detect very small g values in powder spectra due to the large line widths. In the

Table 5
Trigonal Fe(III), Ru(III) and Os(III) complexes with bidentate ligands

Complex	g_{\perp}	g_{\parallel}	$a(t)$	$b(t)$	Δ/ξ	k	Ref.
$[\text{Fe}(\text{en})_3]^{3+}$ *	-2.68	0.60	0.4863	0.8738	1.377	0.959	[32]
	-2.68	-0.60	0.6487	0.7611	0.727	1.090	
$[\text{Fe}(\text{bpy})_3]^{3+}$ *	-2.61	1.61	0.2521	0.9677	3.030	1.068	[33]
	-2.61	-1.61	0.7475	0.6642	0.333	1.230	
$[\text{Fe}(\text{phen})_3]^{3+}$ *	-2.69	1.19	0.3679	0.9299	2.008	0.993	[33]
	-2.69	-1.19	0.7067	0.7076	0.502	1.194	
$[\text{Ru}(\text{en})_3]^{3+}$ *	-2.64	0.33	0.5323	0.8465	1.180	0.947	[34]
	-2.64	-0.33	0.6206	0.7841	0.834	1.025	
$[\text{Ru}(\text{bpy})_3]^{3+}$ *	-2.64	1.14	0.3829	0.924	1.913	0.933	[33]
	-2.64	-1.14	0.7053	0.7089	0.507	1.156	
$[\text{Ru}(\text{phen})_3]^{3+}$ *	-2.63	1.00	0.4143	0.9101	1.731	0.913	[33]
	-2.63	-1.00	0.6928	0.7211	0.557	1.125	
$[\text{Os}(\text{bpy})_3]^{3+}$ *	-2.49	0.40	0.5318	0.8469	1.182	0.829	[33]
	-2.49	-0.40	0.6389	0.7693	0.764	0.940	
$[\text{Os}(\text{phen})_3]^{3+}$ *	-2.43	0.40	0.5360	0.9442	1.165	0.785	[33]
	-2.43	-0.40	0.6430	0.7659	0.749	0.902	
<i>fac</i> - $\text{Os}(\text{PBu}_2\text{Ph})_3\text{Cl}_3$	-1.83	1.28	0.4087	0.9127	1.763	0.156	[15]
*	-1.83	-1.28	0.7736	0.6337	0.216	0.741	

osmium cases the Gaussian line width for g_{\parallel} should be six time greater than that observed for g_{\perp} . It should be noted that Δ is positive for all complexes listed in Table 5. In simple crystal field models a positive Δ means a trigonal elongation from octahedral symmetry.

In every case, except for *fac*-Os(PBu₂Ph)₃Cl₃ we have indicated the favored solution to be the one with the lower k value. Support for this comes from the analysis of the variation of β and Δ/ξ as a function of k using Eqs. (14) and (15). A plot is given in Fig. 1 for [Fe(en)₃]³⁺ for both plus and minus g_{\parallel} values. Similar plots are obtained for the other tris-bidentate complexes. The horizontal line indicates the octahedral value of β . Note that the range of acceptable k values is more acceptable for the favored solution. A more powerful argument for the favored solutions comes from an examination of the change of Δ/ξ for the series Fe, Ru, Os for the same ligand. Δ/ξ decreases as you go down the periodic table for the favored solution and increases for the other solution. Since we could expect Δ to be similar for the triad or at most increase proportional to the crystal field interaction, a decrease in Δ/ξ as we go down the periodic table would be the expected behavior.

In Fig. 2 is plotted Δ/ξ and β as a function of k for Fe, Ru, Os for [M(bpy)₃]³⁺. For k less than that given in Table 5, β increases and Δ/ξ decreases. In these trigonal complexes it is not possible to use AOM arguments like that employed above for tetragonal complexes because in trigonal symmetry it is not easy to separate π and σ bonding interactions. Also, in these bidentate complexes the metal ligand bonds are not 90° due both to the bidentate bite angle being different from 90° and the angle between the bidentate–metal plane and the C₃ axis being different from the 54.7° angle found when all six bonds are 90°. In every case listed in Table 5 Δ/ξ is positive which in the simple crystal field model would imply

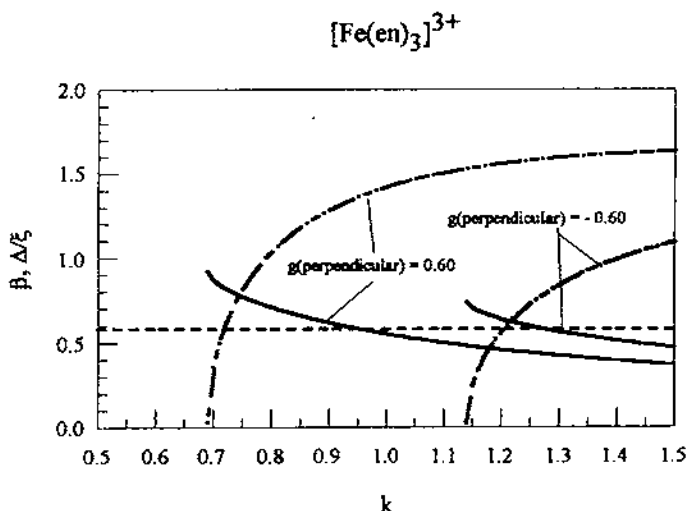


Fig. 1. A plot of the variation of β and Δ/ξ as a function of k for both of the solutions of Eqs. (14) and (15) for [Fe(en)₃]³⁺.

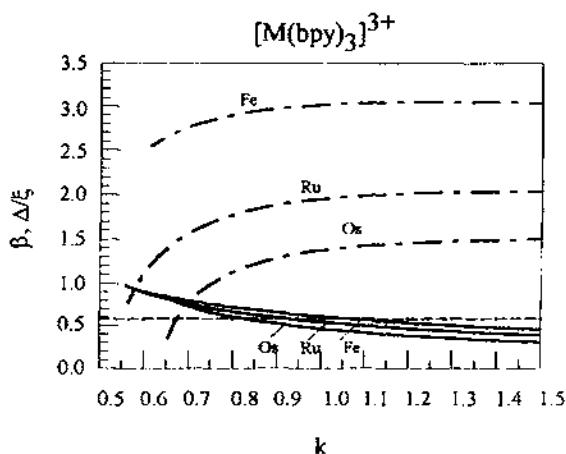


Fig. 2. A plot of Δ/ξ and β as a function of k for $[M(\text{bpy})_3]^{3+}$ where $M = \text{Fe}, \text{Ru}, \text{Os}$.

an “elongation” distortion in which either the bite angle of the bidentate is greater than 90° or the angle between the bidentate–metal plane and the C_3 axis is less than 54.7° due to inter-plane repulsion. The simple point charge model would also favor a smaller value for β when there is such an “elongation” distortion which means that larger values of k than those given in Table 5 should be favored.

4. Conclusions

A systematic comparison of the parameters obtained from the g matrix of strong field d^5 systems has been difficult, due to the use of a variety of different equations, symbols and conventions by various researchers. The requirement that one must choose between 64 combinations of sign and coordinate axes was also discouraging to many. The purpose of this small review is to show that the systematic and simple approach developed earlier [1] for the analysis of the g matrix could be useful for analysis of trends. It is of interest to see how well the AOM approach can account for much of the results obtained from the tetragonally distorted complexes.

The large body of work on heme systems has been left out deliberately to keep the review short. Someone else more closely connected to the field should apply the approach used here to the heme systems.

Acknowledgements

This work was supported in part by an operating grant from the Natural Science and Engineering Research Council of Canada. The original review article and impetus for undertaking this work came during a visit to the Instituto de Química

de São Carlos, Universidade de São Paulo, SP, Brazil, supported by CAPES. The help and hospitality of everyone there is gratefully acknowledged.

References

- [1] B.R. McGarvey, *Quimica Nova* (1998) in press.
- [2] P.H. Rieger, *Coord. Chem. Rev.* 135–136 (1994) 203.
- [3] C.A. Hutchinson Jr., B. Weinstock, *J. Chem. Phys.* 32 (1960) 56.
- [4] C.P.S. Taylor, *Biochim. Biophys. Acta* 491 (1977) 137.
- [5] A. Araneo, G. Mercati, F. Morrazzoni, T. Napoletano, *Inorg. Chem.* 16 (1977) 1196.
- [6] C.E. Schäffer, *Struct. Bonding* 5 (1968) 68.
- [7] C.E. Schäffer, *Theor. Chim. Acta* 4 (1966) 166.
- [8] M. Gerloch, M.R. Manning, *Inorg. Chem.* 20 (1981) 1051.
- [9] E. Larsen, G.N. LaMar, *J. Chem. Educ.* 51 (1974) 633.
- [10] J.M. Baker, B. Bleaney, K.D. Bowers, *Proc. Phys. Soc. London Sect. B* 69 (1956) 1205.
- [11] S. Sakaki, N. Hagiwara, Y. Yanase, A. Ohyoshi, *J. Phys. Chem.* 82 (1978) 1917.
- [12] C. Ezzeh, B.R. McGarvey, *J. Magn. Reson.* 15 (1974) 183.
- [13] D. Kaplan, G. Navon, *J. Phys. Chem.* 78 (1974) 700.
- [14] S. Sakaki, Y. Yanase, N. Hagiwara, T. Takeshita, H. Naganuma, A. Ohyoshi, K. Ohkubo, *J. Phys. Chem.* 86 (1982) 1038.
- [15] A. Hudson, M.J. Kennedy, *J. Chem. Soc. A* (1969) 1116.
- [16] P.T. Manoharan, P.K. Mehrota, M.M. Taqui Khan, R.K. Andar, *Inorg. Chem.* 12 (1973) 2753.
- [17] S. Kremer, *Inorg. Chim. Acta* 85 (1984) 57.
- [18] N.J. Hill, *J. Chem. Soc. Faraday Trans. 2* (1972) 427.
- [19] Y. Kuroda, M. Goto, T. Sakai, *Bull. Chem. Soc. Jpn.* 62 (1989) 3614.
- [20] P. Merrithew, C.C. Lo, A.J. Modestino, *Inorg. Chem.* 14 (1975) 242.
- [21] J.B. Raynor, B.G. Jeliaskowa, *J. Chem. Soc. Dalton Trans.* (1982) 1185.
- [22] A. Desideri, J.B. Raynor, C.-K. Poon, *J. Chem. Soc. Dalton Trans.* (1977) 2051.
- [23] J.B. Raynor, B.G. Jeliaskowa, *J. Chem. Soc. Dalton Trans.* (1982) 1185.
- [24] W. Reiff, R.E. DeSimone, *Inorg. Chem.* 12 (1973) 1793.
- [25] F.A. Walker, D. Reis, V.L. Balke, *J. Am. Chem. Soc.* 106 (1984) 6888.
- [26] C.T. Migita, M. Iwaizumi, *J. Am. Chem. Soc.* 103 (1981) 4378.
- [27] D. Inniss, S.M. Soltis, C.E. Strouse, *J. Am. Chem. Soc.* 110 (1988) 5644.
- [28] M.P. Byrn, B.A. Katz, N.L. Kader, K.R. Levan, C.J. Magurany, K.M. Miller, J.W. Pritt, C.E. Strouse, *J. Am. Chem. Soc.* 105 (1983) 4916.
- [29] S.C. Tang, S. Koch, C.G. Papaefthymiou, S. Foner, R.B. Frankel, J.A. Ibers, R.H. Holm, *J. Am. Chem. Soc.* 98 (1976) 2414.
- [30] J. McKnight, M.R. Cheesman, C.A. Reed, R.D. Orosz, A.J. Thompson, *J. Chem. Soc. Dalton Trans.* (1991) 1887.
- [31] D.J. Kennedy, K.S. Murray, P.R. Zwack, H. Homberg, W. Katz, *Inorg. Chem.* 25 (1986) 2539.
- [32] R.E. De Simone, *J. Am. Chem. Soc.* 95 (1973) 6238.
- [33] R.E. De Simone, R.S. Drago, *J. Am. Chem. Soc.* 92 (1970) 2343.
- [34] J.A. Stanko, H.J. Peresie, R.A. Bernheim, R. Wang, P.S. Wang, *Inorg. Chem.* 12 (1973) 634.